# 1 Tables

S 1: Models overview.

| Model | Horizontal resolution (lat x lon) | Vertical resolution (model top, # levels) | Reference |
|---|---|---|---|
| ECHAM6-SALSA | 1.9°x 1.9°(T63) | 0.01 hPa, 95 levels | Kokkola et al. (2018) and Laakso et al. (2017) |
| ECHAM5-HAM | 2.8°x 2.8°(T42) | 0.01 hPa, 90 levels | Niemeier et al. (2009) and Toohey et al. (2013b) |
| EMAC | 1.9°x1.9°(T63) | 0.01 hPa, 90 levels | Jöckel et al, (2010), Brühl et al. (2018) |
| SOCOL-AERv2 | 2.8°x 2.8°(T42) | 0.01 hPa, 39 levels | Sheng et al. (2015) and Sukhodolov et al. (2018) |
| ULAQ-CCM | 5°x 6°(T21) | 0.04 hPa, 126 levels | Pitari et al. (2016) and Visioni et al. (2018) |
| UM-UKCA | 1.25°x 1.875°(N96) | 80 km, 85 levels | Dhomse et al. (2014) and Marshall et al. (2019) |

S 2: Peak value of the global stratospheric sulfate burden (in Tg-S), month in which it is reached since January 1991 and e-folding time for each model and experiment.

| | Low-22km | | | Med-22km | | | High-22km | | | Med-19km | | | Med-18-25km | | |
|---|---|---|---|---|---|---|---|---|---|---|---|---|---|---|---|
| Model | Peak | Month | e-fold | Peak | Month | e-fold | Peak | Month | e-fold | Peak | Month | e-fold | Peak | Month | e-fold |
| ECHAM6-SALSA | 4.8 | 10 | 10 | 6.7 | 10 | 11 | 9.5 | 11 | 12 | 6.1 | 10 | 9 | 6.7 | 10 | 13 |
| ECHAM5-HAM | 5.0 | 12 | 11 | 7.0 | 12 | 10 | 9.9 | 12 | 9 | 6.0 | 10 | 11 | 6.5 | 11 | 11 |
| EMAC | | | | 7.0 | 9 | 8 | | | | | | | | | |
| SOCOL-AERv2 | 4.8 | 10 | 14 | 6.6 | 10 | 13 | 9.4 | 10 | 13 | 5.4 | 9 | 13 | 6.6 | 10 | 14 |
| ULAQ-CCM | 5.0 | 11 | 13 | 7.0 | 11 | 13 | 9.8 | 11 | 12 | 6.6 | 11 | 10 | 6.9 | 11 | 13 |

# 2 Figures

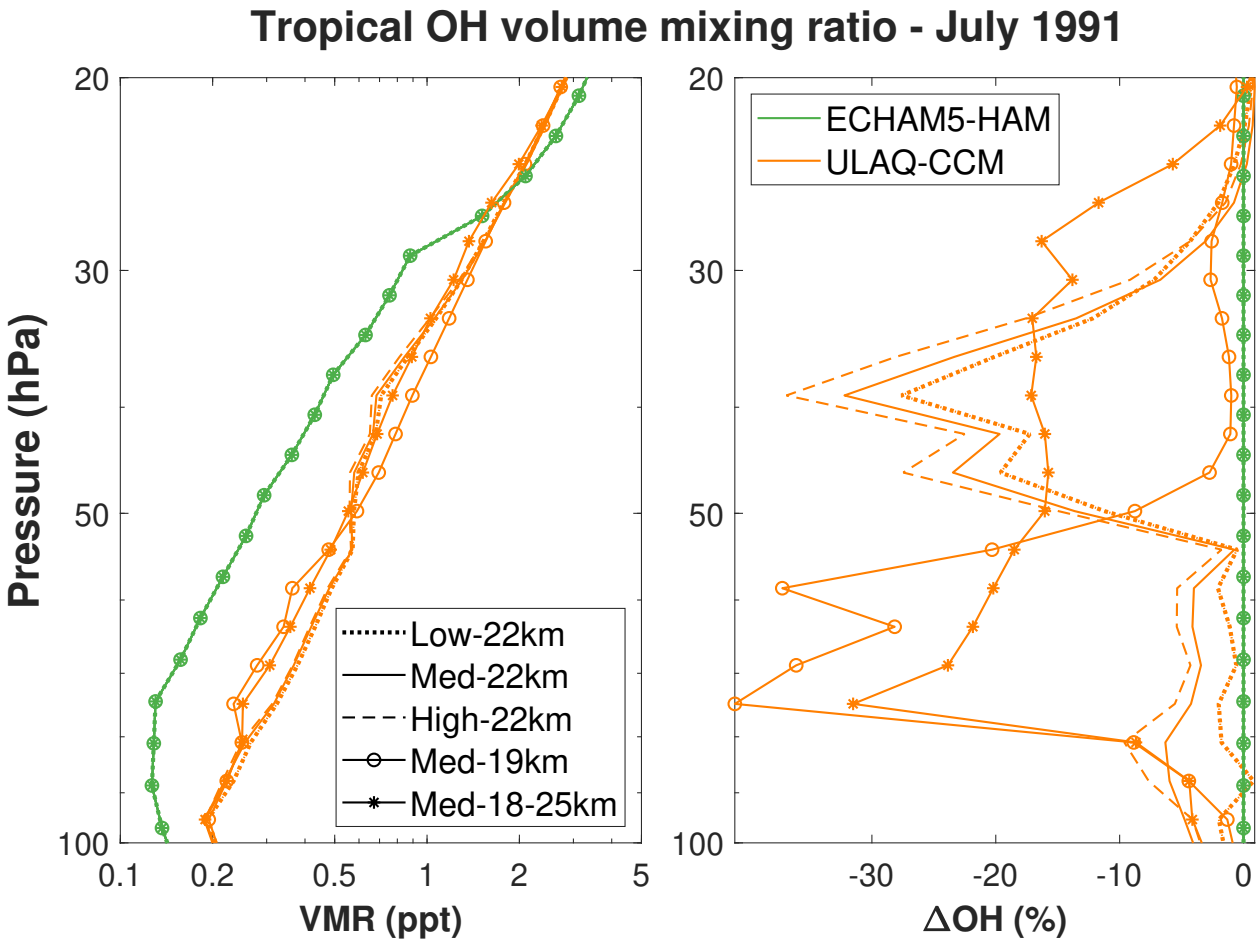


S 1: Vertical distribution of OH mixing ratio in July 1991 and its change compared to background condition (July 1991 without eruption) in ECHAM5-HAM (prescribed OH) and ULAQ-CCM (interactive OH).

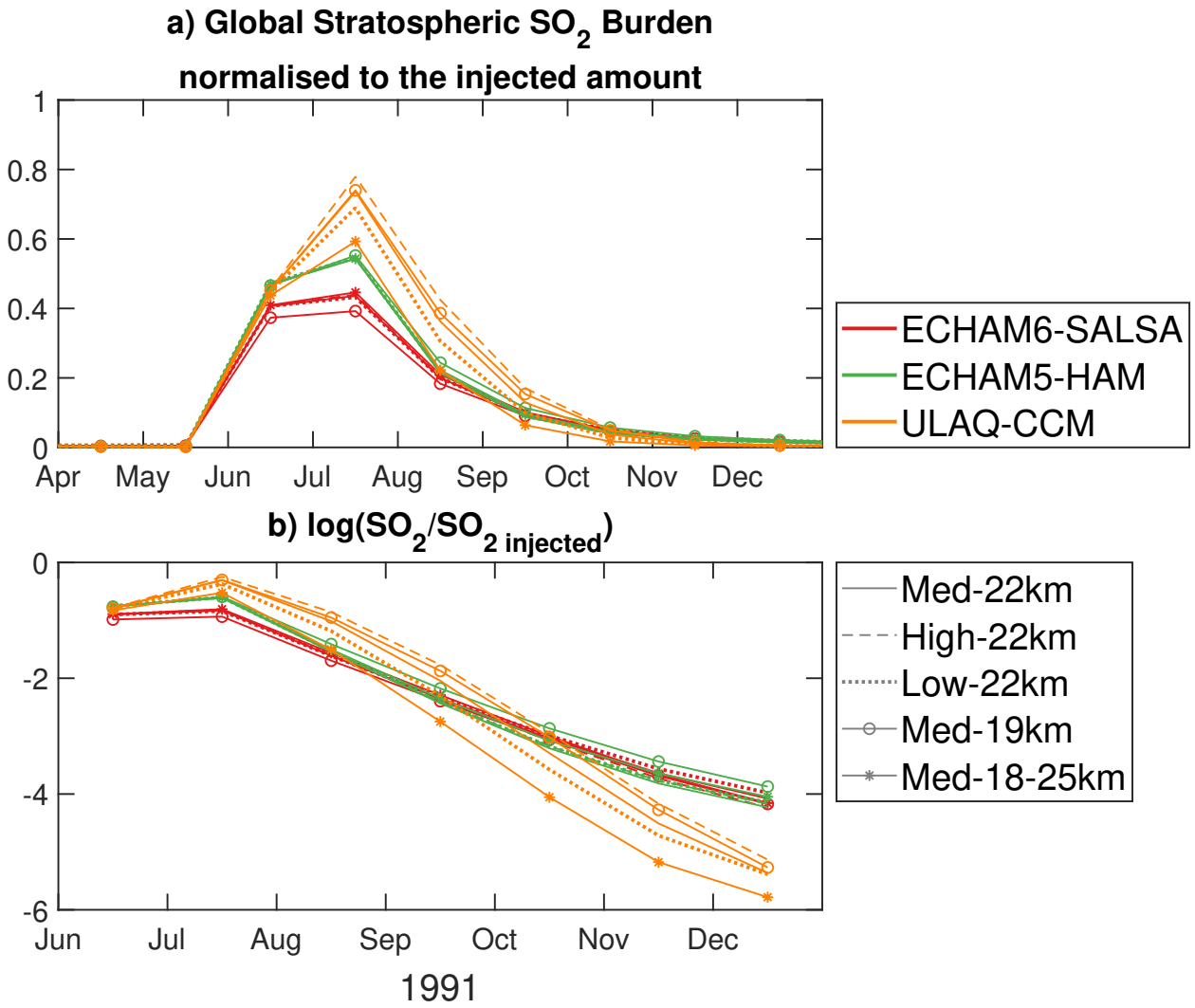


S 2: Time evolution of global stratospheric $SO_2$ burden in Tg-S (a) and logarithm of $SO_2$ burden divided by the amount of $SO_2$ injected (b) in all model experiments. The models are identified by the different colours (top legend), the different scenarios by the different line styles (bottom legend).

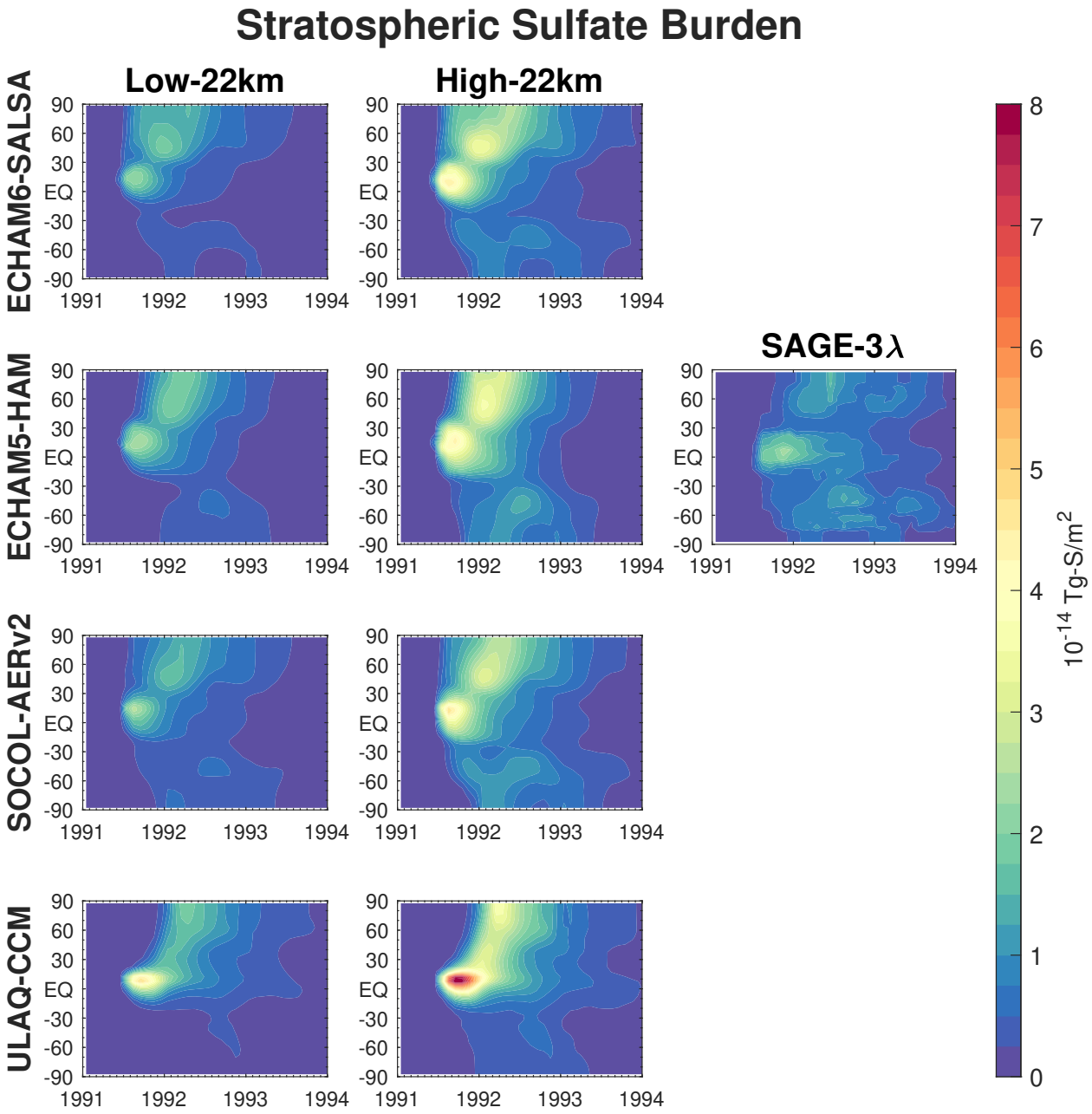


S 3: Time evolution of zonal stratospheric sulfate burden (in $10^{-14}$ Tg-S/m$^2$) in Low-22km (first column) and High-22km (second column) for all models, and zonal stratospheric sulfate burden of SAGE-3$\lambda$ (third column).

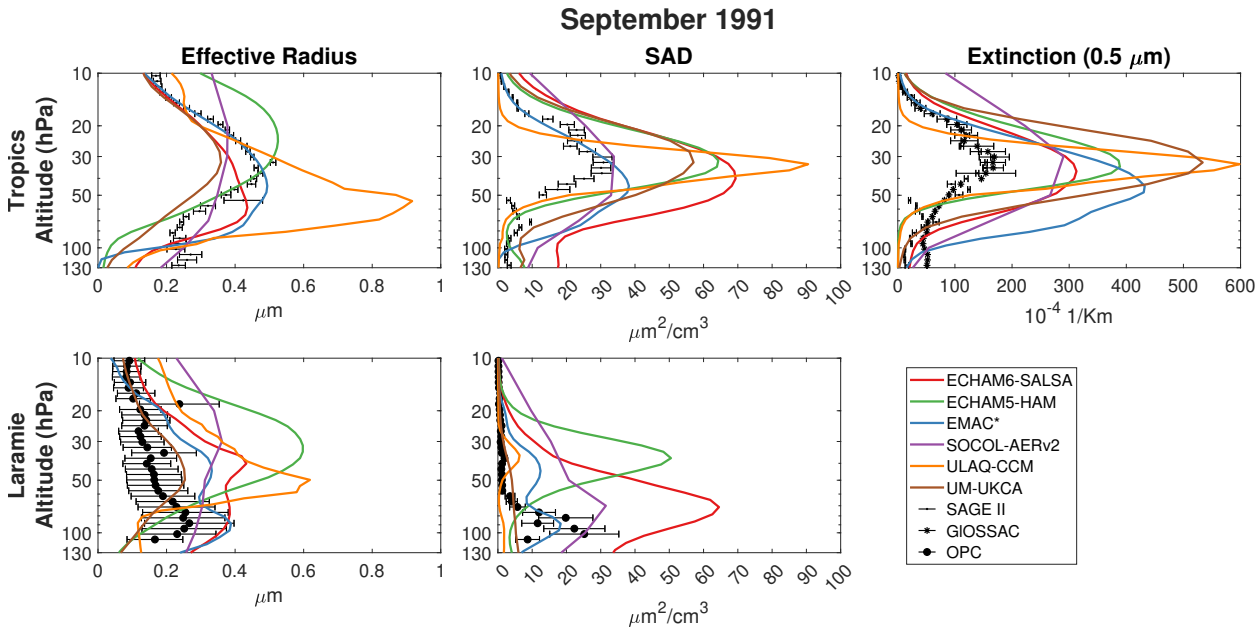


S 4: Vertical profile of the effective radius in $\mu$m (left panels), surface area density (SAD) in $\mu m^2/cm^3$ (middle panels), and extinction at 0.5 $\mu$m in 1/km (right panel) in the tropics (first row) and over Laramie (second row) for Med-22km in September 1991. Model results are compared with SAGE II and GloSSAC in the tropics and with OPC over Laramie.

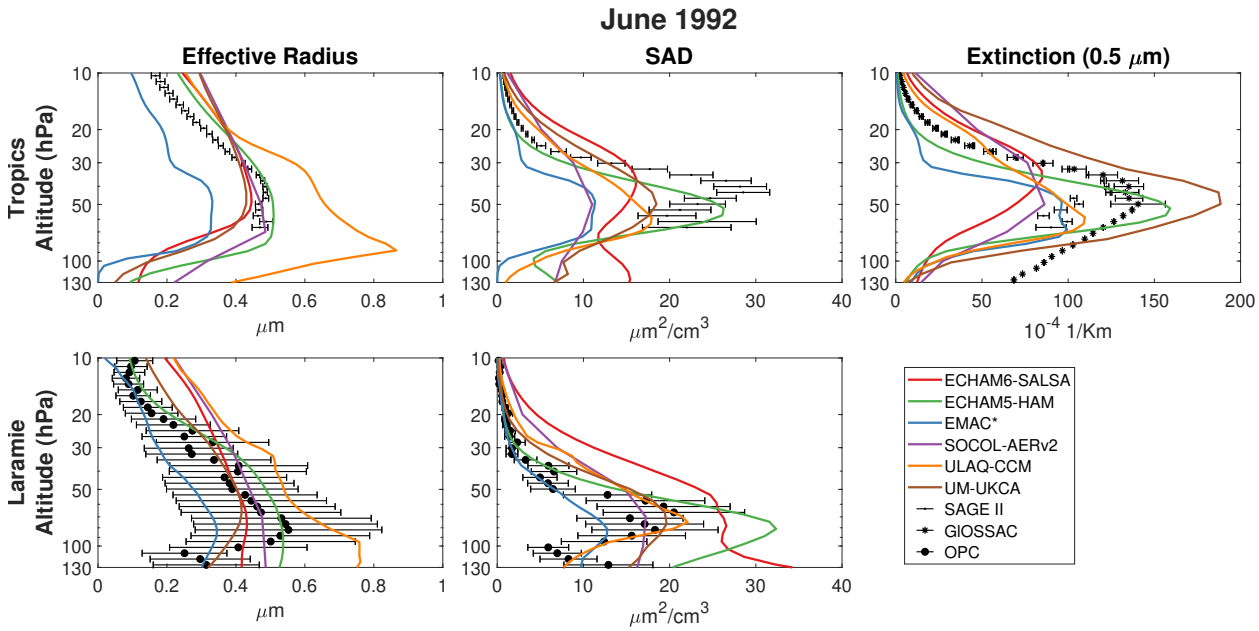


S 5: Vertical profile of the effective radius in $\mu$m (left panels), surface area density (SAD) in $\mu m^2/cm^3$ (middle panels), and extinction at 0.5 $\mu$m in 1/km (right panel) in the tropics (first row) and over Laramie (second row) for Med-22km in June 1992. Model results are compared with SAGE II and GloSSAC in the tropics and with OPC over Laramie.

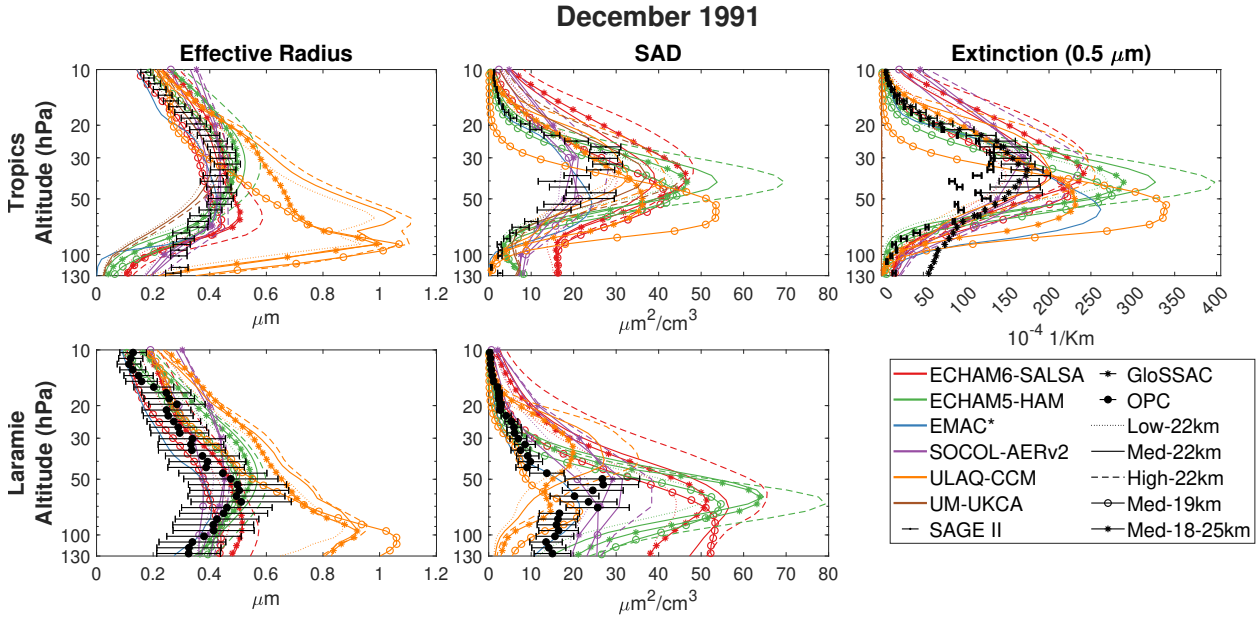


S 6: Vertical profile of the effective radius in $\mu$m (left panels), surface area density (SAD) in $\mu m^2/cm^3$ (middle panels), and extinction at 0.5 $\mu$m in 1/km (right panel) in the tropics (first row) and over Laramie (second row) for all experiments in December 1991. Model results are compared with SAGE II and GloSSAC in the tropics and with OPC over Laramie.

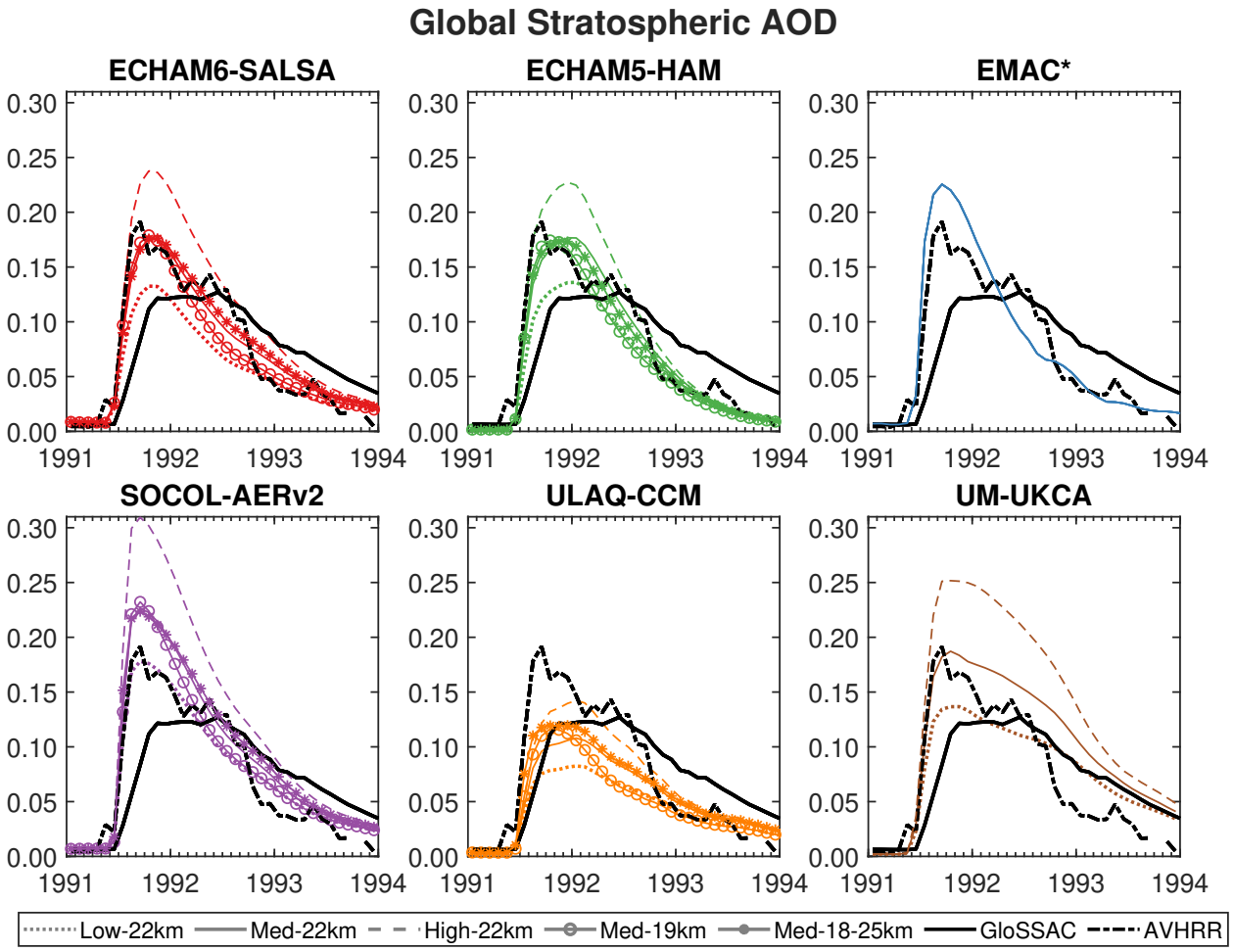


S 7: Temporal evolution of monthly global stratospheric AOD values. Each panel refers to the respective model in which the results of the different experiments (coloured lines; different line styles are used for the different experiments, see legend on the left) are compared to the GloSSAC and AVHRR measurements (black lines).